

Intercomparison of whole-body averaged SAR in European and Japanese voxel phantoms

Peter J Dimbylow¹, Akimasa Hirata² and Tomoaki Nagaoka³

¹Radiation Protection Division, Health Protection Agency, Chilton, Didcot, OX11 0RQ
peter.dimbylow@hpa.org.uk

²Nagoya Institute of Technology, Gokiso-cho, Showa-ku, 466-8555 Nagoya, Japan
ahirata@nitech.ac.jp

³Electromagnetic Compatibility Group, Applied Electromagnetic Research Center, National Institute of Information and Communications Technology, Nukuikitamachi 4-2-1, Koganei, Tokyo 184-8795, Japan
nagaoka@nict.go.jp

Abstract

This paper provides an intercomparison of the HPA male and female models, NORMAN and NAOMI with the National Institute of Information and Communications Technology (NICT) male and female models, TARO and HANAKO. Calculations of the whole-body SAR in these 4 phantoms were performed at the HPA, at NICT and at the Nagoya Institute of Technology (NIT). These were for a plane wave with a vertically aligned electric field incident upon the front of the body from 30 MHz to 3 GHz for isolated conditions. As well as investigating the general differences through this frequency range, particular emphasis was placed on the assumptions of how dielectric properties are assigned to tissues (particularly skin and fat) and the consequence of using different algorithms for calculating SAR at the higher frequencies.

1. Introduction

At radiofrequencies, the ICNIRP (1998) electromagnetic field guidelines restrict exposure to limit the temperature rise in the body. The whole-body averaged specific energy absorption rate, SAR is used as a surrogate measure to quantify the body-core temperature rise. However, SAR is a difficult quantity to measure. Calculations in realistic models of the body are used to link SAR to external field values and sources which are more readily measured or characterised. Anatomically realistic models of the human body are derived from medical imaging scans and have typically voxel resolutions of 1 to 2 mm (e.g. Dimbylow 1997, 2005a; Nagaoka *et al* 2004, 2007). Calculations of the SAR as a function of frequency in a particular voxel model will give an indication of the link between external field values and the whole-body SAR and also to whether external field reference levels are high enough such that limits on the SAR will not be exceeded (Dimbylow 2002, 2005b, 2007; Findlay *et al* 2006a, 2008; Hirata *et al* 2007, Nagaoka *et al* 2004, Wang *et al*, 2006). There are two main factors influencing calculated whole-body average SAR. One is the computational uncertainty, such as in boundary conditions (Findlay *et al* 2006a) and dielectric properties definition, etc. The other is the model variability, such as different heights, masses, ethnic background, organ definitions and properties (Conil *et al* 2008). This analysis will focus on what elements are the most important in the calculation of SAR and indicate the levels of uncertainty in the definition of external field reference levels via the intercomparison of three laboratories.

This paper provides an intercomparison of the HPA male and female models, NORMAN and NAOMI with the National Institute of Information and Communications Technology (NICT) male and female models, TARO and HANAKO. Calculations of the whole-body SAR in these 4 phantoms were performed at the HPA, at NICT and at the Nagoya Institute of Technology (NIT). Calculations were performed for a plane wave with a vertically aligned electric field incident upon the front of the body from 30 MHz to 3 GHz for isolated conditions. As well as investigating the general differences through this frequency range, particular emphasis was made on the assumptions of how dielectric properties are assigned to tissues (particularly skin and fat) and the consequence of using different algorithms for calculating SAR at the higher frequencies.

2. Voxel models

2.1. TARO and HANAKO

A full description of the development of the Japanese adult male and female voxel models, TARO and

HANAKO is given in Nagaoka *et al* (2004). The average height and weight of Japanese 18 to 30 years old are 1.714 m and 63.3 kg for males, and 1.591 m and 52.6 kg for females (NIBH 1996). Volunteers were selected whose dimensions were close to the average values. The male volunteer was 22-years old, 1.728 m tall and weighed 65.0 kg; the female volunteer was 22-years old, 1.6 m tall and weighed 53.0 kg. A complete set of MRI 256 x 256 axial images with a 240 mm field-of view (FOV) for a head and a 480 mm FOV for other parts of the body was acquired at a slice thickness of 2 mm. The voxels were rescaled to 2 mm cubes and segmented to define 51 discrete organs.

2.2. NORMAN and NAOMI

The Health Protection Agency (formerly the NRPB) male phantom is known as NORMAN (Dimbylow 1997). The phantom was normalised to be 1.76 m tall and to have a mass of 73 kg, the values for ICRP reference man (ICRP, 2002). Hence, the name was derived from NORMalised MAN and the phantom is meant to represent the anatomy and size of an average or reference man. The height fixes the vertical voxel dimension, 2.021 mm, and the horizontal dimensions, 2.077 mm, are then fixed by the mass. The model was derived from a series of continuous partial body MRI scans of a single subject. The greyscale data were interpreted into 37 tissue types. The total domain of the phantom and adjacent air is a 3D array of 148 voxels from front to back, 277 from side to side and 871 voxels high. There are 8.3 million voxels in the body.

The development of the female voxel model, NAOMI is described in detail in Dimbylow (2005). The primary medical imaging data were derived from a high-resolution MRI scan of a 1.65 m tall, 23 year-old female subject with a mass of 58 kg. The model was rescaled to a height of 1.63 m and a mass of 60 kg, the dimensions of the ICRP reference adult female (ICRP, 2002). The 8-bit grey-scale images were segmented unambiguously as belonging to one of 41 different tissue types. In NORMAN, the brain was treated as one tissue type. In this female model the grey and white matters were differentiated separately. The reference female is 1.63 m tall and weighs 60 kg. There are 791 slices in the body so the vertical voxel dimension is 2.061 mm. The horizontal dimensions, 1.948 mm, are then fixed by the mass.

3. SAR calculations

3.1 TARO and HANAKO

Finite-Difference Time-Domain (FDTD) calculations (see e.g. Taflov, 1995) have been performed from 30 MHz to 3 GHz for a plane wave with a vertically aligned electric field. The body is isolated and the field propagation direction is into the front of the body. The HPA and NICT programs use the split-field, perfectly

matched layer (pml) based boundary conditions (Berenger, 1994). The NIT program uses the uniaxial formulation, upml (Gedney, 1996). The evaluated review of the dielectric properties of all the tissue types in the body by Gabriel (1995, 1996a-c) was used. However, in their calculations the three institutes made different assumptions about how the properties in the review were assigned to the different tissues in the models. Table 1 compares the whole-body averaged SAR values in TARO and HANAKO from NICT, NIT and HPA calculated at a resolution of 2 mm. The HPA calculations endeavoured to make the same assumptions about assigning the Gabriel dielectric data to the various tissue types as used in the NICT calculations. In particular, the skin parameters were taken to be an average of wet and dry skin and the lung values were taken to be an average of inflated and deflated lung. However, different tissue densities were used in the three institutes. The NIT densities give a mass of 65.66 kg, the NICT densities give a mass of 67.76 kg and the HPA densities give a mass of 63.98 kg for TARO. The whole-body averaged SAR is the total energy absorption rate in the body divided by the total mass of the body. This quantity does not depend on how the individual organ densities are defined but just on the total mass. Therefore the SAR values were all normalised to 65 kg, the Japanese male reference mass. Similarly, the HANAKO SAR values were normalised to 53 kg, the Japanese female reference mass. The HPA calculations used a boundary separation of up to 4 cells and the pml layer consisted of 12 cells. The NICT calculations used a 100 cell gap and a pml layer of 8 cells. The NIT calculations used a 50 cell gap and an upml layer of 12 cells.

Figure 1 plots the whole-body averaged SAR for TARO and figure 2 displays the percentage differences of the NICT and NIT calculations from the HPA whole-body averaged SAR values normalised to 65 kg. Figure 3 plots the whole-body averaged SAR for HANAKO and figure 4 displays the percentage differences of the NICT and NIT calculations from the HPA whole-body averaged SAR values normalised to 53 kg. Looking at the comparisons between the three laboratories there seems to be very good agreement when the calculations have been normalised to the same mass even though using different absorbing boundary conditions. The differences of the NICT and NIT calculations from HPA are generally less than ~5 %. However, an interesting point is that the HPA calculations at the highest frequencies are noticeably lower than the two others, a feature that will be discussed later in the following sections.

3.2 *NORMAN and NAOMI*

Figure 5 gives a comparison between NAOMI and HANAKO for the HPA calculations using the reference masses and figure 6 gives a similar comparison between NORMAN and TARO. The NICT models are slightly shorter than the HPA models but there is no significant upward shift in the resonant frequency. The Japanese models produce systematically higher SAR values than NORMAN and NAOMI due to their different anatomical composition and probably more importantly because of their smaller mass in the SAR

quotient. As well as basic individual anatomical differences there are differences in the way dielectric properties are assigned. The main differences are that in the NICT models skin is taken to be an average of the wet and dry skin properties and the values for lung are taken as an average of inflated and deflated properties. In the HPA models the wet skin properties are used and the values for lung are taken to be 1/3 lung tissue and 2/3 air, also the small intestine includes a proportion of contents as well as the intestinal wall.

Table 2 compares the whole-body averaged SAR values for NORMAN (normalised to 73.01 kg) and NAOMI (normalised to 59.88 kg). Figure 7 plots the whole-body averaged SAR for NORMAN and figure 8 displays the percentage differences of the NIT and NICT calculations from the HPA whole-body averaged SAR values. Similarly, figure 9 plots the whole-body averaged SAR for NAOMI and figure 10 displays the percentage differences of the NIT and NICT calculations from the HPA whole-body averaged SAR values. The NORMAN data are consistent below ~ 1 GHz but above this frequency the NIT and NICT calculations diverge away from those of the HPA. A similar pattern at the high frequencies can be seen in NAOMI. Also in the female model there is a variance between the NIT and NICT calculations at and below resonance where the SAR value is changing rapidly with frequency. The divergence at the higher frequencies could be due to the boundary conditions used, the definition of tissue properties or the type of algorithm used in defining SAR. The latter two proposals are investigated in the following sections. Findlay *et al* (2006b) showed that there is negligible variation in the whole-body averaged SAR values, calculated between 70 MHz and 3 GHz, when the distance between the voxel phantom and pml absorbing boundaries was increased above a separation of 2 cells. This finding was also confirmed by Laakso *et al* (2007).

3.3 *Influence of dielectric properties*

One possible reason why the NICT and NIT calculations diverge from the HPA values in NORMAN and NAOMI at the higher frequencies is because of differing assumptions on the way in which the Gabriel *et al* dielectric property values are assigned to different tissues, e.g. the NICT/NIT calculations assign an average of the wet and dry skin properties to the skin voxels whilst the HPA uses the properties of wet skin. This assumption was made because the values for dry skin can vary noticeably from person to person and depend critically on the thin surface layer. The values for wet skin are far more consistent and represent better the bulk properties of skin and the subcutaneous layer. The dielectric properties of the skin voxels and also the subcutaneous fat can have a significant effect at the higher frequencies as the energy absorption becomes more superficial and the effects of surface reflection become more important. A sensitivity analysis was performed of the skin and subcutaneous fat properties on the whole-body averaged SAR in NORMAN from 0.4 to 3 GHz. Six combinations were tested, 3 values for the skin voxels with 2 values for the fat voxels. The

skin voxels were set to (a) wet skin, (b) an average of wet and dry skin, (c) dry skin. The fat voxels were set either to fat infiltrated with blood or fat not infiltrated with blood. The standard properties for fat voxels were those for which fat is infiltrated with blood but the effect of using the values for fat not infiltrated with blood was also tested. The standard HPA properties in NORMAN are wet skin with fat infiltrated with blood. Table 3 gives the SAR values for the 6 combinations of skin and fat properties. Figure 11 shows the percentage differences from the standard case (fat infiltrated with blood and wet skin) of the other 5 combinations. The general trend is for SAR to increase with the lower conductivity properties, possibly due to less reflection of the incident field from the surface of the body (Dimbylow, 2005b). The highest SAR values occur for fat not infiltrated with blood and dry skin. Table 4 compares the results from the 3 institutes for these 6 combinations of skin and fat properties at 1800 MHz. Again the same general trend can be seen but the absolute values of the NICT and NIT results are still higher than the HPA values.

3.4 SAR algorithms

The other possible reason for the differences in the SAR values at the higher frequencies is thought to be the method of evaluating SAR from the electric field values. The standard way the HPA code calculate SAR is as follows. At each time step the average of E_x (and E_y and E_z) is calculated from the 4 edges of the Yee cell to obtain the field components at the centre of the voxel. These components are then squared and summed to produce $|E^2|$ at that time step. The maximum value of this quantity is then sought over a half-period of the wave to produce the SAR for that voxel. Let this method be denoted algorithm A. As a fundamental study, various other methods have been looked at. E.g. change the standard method so that at each time step the squared values E_x^2 (and E_y^2 and E_z^2) are calculated on each edge of the Yee cell. An average value of E_x^2 is then calculated at the centre of the voxel. The averaged square values for the components are then summed to produce $|E^2|$ at that time step. The maximum value of this quantity is then sought over a half-period of the wave to produce the SAR. Call this algorithm B. Instead of constructing the SAR as a function of time in each voxel one could, over the half-period, calculate the maximum absolute value of E_x , E_y and E_z separately at all voxel edges in the model. These can then be combined by using either algorithm C (as used by NICT) : – average $|E_x|$ (and $|E_y|$ and $|E_z|$) from the 4 edges to obtain the field at the centre of the voxel, which is then squared to find the SAR or by algorithm D: – average $|E_x^2|$ (and $|E_y^2|$ and $|E_z^2|$) from the 4 edges to obtain the averaged square fields at the centre of the voxel which are then added to obtain the SAR. The two latter methods will provide a conservative estimate because they assume that all the three field components are in phase. Table 5 gives HPA calculations of the SAR from 0.1 to 3 GHz in NORMAN for these 4 algorithms and figure 12 plots the percentage differences from the standard algorithm A. The divergence between the methods increases with frequency. E.g. at 3 GHz algorithm C produces SAR values

15.5 % higher than the standard algorithm. Table 6 compares HPA, NICT and NIT SAR values at 900, 1800 and 3000 MHz for NAOMI using the same assumptions about dielectric properties and employing the standard algorithm A. Now the residual differences between the 3 institutes are much less significant and can be ascribed to the use of different compilers, computers, and the particular implementations of the FDTD method in the institute's codes.

4. Discussion

One has to be careful in making facile comparisons between raw sets of SAR data from different laboratories using different models, material properties and numerical methods. The three institutes used different sets of tissue densities. The whole-body averaged SAR is the total energy absorption rate in the body divided by the total mass of the body. This quantity does not depend on how the individual organ densities are defined but just on the total mass. Therefore, a direct comparison can be made between the three sets of calculations by first normalising the SAR values to a standard mass. In the comparisons on the NICT models, TARO and HANAKO, the HPA calculations endeavoured to make the same assumptions about assigning the Gabriel dielectric data to the various tissue types as used in the NICT model. In particular, the skin parameters were taken to be an average of wet and dry skin and the lung values were taken to be an average of inflated and deflated lung. Looking at the comparisons between the three laboratories there seems to be very good agreement, the differences of the NICT and NIT calculations from HPA are generally within ~5 % except at the highest frequencies.

The NORMAN and NAOMI comparisons are similarly consistent below ~ 1 GHz but above this frequency the NIT and NICT calculations again diverge away from those of the HPA. It has been suggested by Wang *et al* (2006) that this divergence could be due to the different separations from the body to the pml boundary layers. However, Findlay *et al* (2006b) showed that there is negligible variation in the whole-body averaged SAR values, calculated between 70 MHz and 3 GHz, when the distance between the voxel phantom and pml absorbing boundaries was increased above a separation of 2 cells. The dielectric properties of the skin voxels and also the subcutaneous fat can have a significant effect at the higher frequencies as the energy absorption becomes more superficial and the effects of surface reflection become more important. However the difference due to the HPA assumption that wet skin properties should be used for the skin voxels as opposed to the NICT/NIT assumption that the skin voxels should have the average properties of wet and dry skin made a small difference of a few percent. The main difference between the sets of calculations was

found to be in which the SAR in each voxel was derived from the field values. The method used in the HPA calculations is to average the field components in the Yee grid at each time step to obtain their values at the centre of the voxel. These components are then squared and summed to produce $|E^2|$ at that time step. The maximum value of this quantity is then sought over a half-period of the wave to produce the SAR for that voxel. Alternatively, the maximum absolute value of E_x , E_y and E_z can be calculated separately at all voxel edges over a half-period and then the SAR is constructed afterwards in each voxel. This latter method will provide a conservative estimate because it makes the approximation that all the three field components are in phase. When the three institutes used the same assumptions about dielectric properties and employed the first method to calculate SAR, the differences between the calculations at the higher frequencies were much less significant.

5. Conclusions

FDTD calculations of the whole-body averaged SAR in two male and two female phantoms were performed at the HPA, at NICT and at NIT for a plane wave with a vertically aligned electric field incident upon the front of the body from 30 MHz to 3 GHz for isolated conditions. This paper investigated what elements are the most important in the calculation of SAR and reveal the levels of uncertainty in the definition of external field reference levels via inter-comparison of three institutes. The main factors influencing the whole-body average SAR are the dielectric parameters, especially of the skin and fat and the SAR averaging scheme for frequencies above 1 GHz. Good agreement was found in the whole-body averaged SAR when the same dielectric parameters and SAR averaging algorithms are used.

Acknowledgements

The authors would like to thank Prof. Osamu Fujiwara of NIT and Prof. Soichi Watanabe of NICT for their support and encouragement.

References

- Berenger, J, 1994. A perfectly matched layer for the absorption of electromagnetic waves. *J. Comp. Phys.* **114**, 185-200.
- Conil E, Hadjem A, Lacroux F, Wong M F and Wiart J, 2008. Variability analysis of SAR from 20 MHz to 2.4 GHz for different adult and child models using finite-difference time-domain. *Phys. Med. Biol.* **53** 1511-25.
- Dimbylow P J, 1997. FDTD calculations of the whole-body averaged SAR in an anatomically realistic voxel model of the human body from 1 MHz to 1 GHz. *Phys. Med. Biol.* **42** 479-90.
- Dimbylow P J, 2002. Fine resolution calculations of SAR in the human body for frequencies up to 3 GHz. *Phys. Med. Biol.* **47** 2835-46.
- Dimbylow P J, 2005a. Development of the female voxel phantom, NAOMI and its application to calculations of induced current densities and electric fields from applied low frequency magnetic and electric fields. *Phys. Med. Biol.* **50** 1047-70.
- Dimbylow P J., 2005b. Resonance behaviour of whole-body averaged specific energy absorption rate (SAR) in the female voxel model, NAOMI. *Phys. Med. Biol.* **50** 4053-63.
- Dimbylow P J., 2007. SAR in the mother and foetus for RF plane wave irradiation. *Phys. Med. Biol.* **52** 3791-3802.
- Findlay R P and Dimbylow P J., 2006a. FDTD calculations of specific energy absorption rate in a seated voxel model of the human body from 10 MHz to 3 GHz. *Phys. Med. Biol.* **51** 2339-2352.
- Findlay R P and Dimbylow P J, 2006b. Variations in calculated SAR with distance to the perfectly matched layer boundary for a human voxel model. *Phys. Med. Biol.* **51** N411-5.
- Findlay R P and Dimbylow P J, 2008. Calculated SAR distributions in a human voxel phantom due to the reflection of electromagnetic fields from a ground plane between 65 MHz and 2 GHz. *Phys. Med. Biol.* **53** 2277-89.
- Gabriel C, 1995. Compilation of the dielectric properties of body tissues at RF and microwave frequencies *Report prepared for the NRPB by Microwave Consultants Ltd.*
- Gabriel C, Gabriel S, and Corthout E, 1996a. The Dielectric properties of biological tissues: 1. Literature Survey *Phys. Med. Biol.* **41** 2231-2249.
- Gabriel S, Lau R W, and Gabriel C 1996b. The Dielectric properties of biological tissues: 2. Measurements in the frequency range 10 Hz to 20 GHz *Phys. Med. Biol.* **41** 2251-2269.
- 1996c. The Dielectric properties of biological tissues: 3. Parametric models for the dielectric spectrum of tissues. *Phys. Med. Biol.* **41** 2271-2293.
- Gedney S D, 1996. An isotropic perfectly matched layer absorbing boundary medium for truncation of FDTD lattices. *IEEE Trans. Antennas Propag.* **44** 1630-9.
- Hirata A, Kodera S, Wang J and Fujiwara, 2007. Dominant factors influencing whole-body average SAR due to far-field exposure in whole-body resonance frequency and GHz regions. *Bioelectromagnetics* **28** 484-7.
- ICNIRP, 1998. Guidelines for limiting exposure to time-varying electric, magnetic and electromagnetic fields (up to 300 GHz). *Health Physics* **74** (4), 494-522.
- ICRP, 2002. Publication 89 32(3-4) ISSN 0146-6453 Basic anatomical and physiological data for use in radiological protection: reference values.
- Laakso I, Ilvonen and Uusitupa T, 2007. Performance of convolutional PML absorbing boundary conditions in finite-difference time-domain SAR calculations. *Phys. Med. Biol.* **52** 7183-92.
- NIBH 1996 *Human Body Dimensions Data for Ergonomic Design* (Tokyo: Research Institute of Human Engineering for Quality Life)

Nagaoka T, Watanabe S, Sakurai K, Kunieda E, Watanabe S, Taki M and Yamanaka Y, 2004. Development of realistic high-resolution whole-body voxel models of Japanese adult males and females of average height and weight and application of models to radio-frequency electromagnetic-field dosimetry. *Phys. Med. Biol.* **49** 1-15.

Nagaoka T, Togashi T, Saito K, Takahashi M, Ito K and Watanabe S, 2007. An anatomically realistic whole-body pregnant-woman model and specific absorption rates for pregnant-woman exposure to electromagnetic plane waves from 10 MHz to 2 GHz. *Phys. Med. Biol.* **52** 6731-45.

Taflov A 1995 *Computational Electromagnetics – the Finite-Difference Time-Domain Method* (London: Artech)

Wang J, Fujiwara O, Kadera S and Watanabe S, 2006. FDTD calculation of whole-body average SAR in adult and child models for frequencies from 30 MHz to 3 GHz *Phys. Med. Biol.* **51** 4119-27.

Table 1. Whole-body averaged SAR values, $\mu\text{W kg}^{-1}$ at 2 mm resolution. The values for TARO are normalised to 65 kg and those for HANAKO are normalised to 53 kg. The incident electric field is 1 V m^{-1} (r.m.s.).

MHz	TARO			HANAKO		
	NIT	NICT	HPA	NIT	NICT	HPA
30	16.20	15.97	15.96	15.30	15.29	15.18
40	32.63	33.26	32.20	29.14	30.24	28.42
50	57.73	55.45	56.93		48.51	48.10
60	84.17	78.84	82.78		69.67	70.38
65			89.44			86.25
70	91.19	88.33	89.38	87.97	86.23	87.69
80	78.00	76.21	75.58	87.25	86.94	84.93
90	61.19	60.32	59.66	74.81	74.87	72.56
100	48.53	47.71	48.11	60.66	60.53	59.24
120	34.86	34.28	34.82		41.25	40.98
150		27.37	28.12		30.21	30.24
180		25.46	25.63		27.23	27.46
200	25.90	25.15	24.68	27.31	26.94	26.53
300	19.84	18.87	19.25		21.76	21.58
400	19.92	18.82	18.92	21.55	20.80	20.21
500	19.76	18.87	18.86		21.73	21.27
600	19.20	18.82	18.71	22.46	22.54	22.00
700	18.45	18.87	18.81		22.67	22.09
800	18.96	19.43	19.36	22.57	23.36	22.76
900	19.39	19.67	19.57		23.43	23.01
1000	20.16	19.95	19.84	23.33	23.61	22.96
1200	19.92		20.34	23.64		22.66
1400			19.93			
1500	20.46		19.64	22.51		21.42
1800	19.90		18.74	20.81		19.75
2000	19.71	18.76	17.94	19.66	19.79	18.50
2450			16.01			16.21
3000	14.48	15.90	13.54	15.55	16.78	14.19

Table 2. Whole-body averaged SAR values, $\mu\text{W kg}^{-1}$ at 2 mm resolution. The values for NORMAN are normalised to 73.01 kg and those for NAOMI are normalised to 59.88 kg. The incident electric field is 1 V m^{-1} (r.m.s.).

MHz	NORMAN			NAOMI		
	NIT	NICT	HPA	NIT	NICT	HPA
30	16.98	17.78	17.12			13.61
40	32.72	34.51	33.22	23.88	27.56	25.58
50	55.48	54.68	55.65	40.03	44.42	43.66
60	76.25	75.12	76.34	60.29	63.68	64.45
65	81.19		80.28			73.03
70	80.49	80.69	79.23	75.73	78.67	78.38
75						79.05
80	68.91	69.28	67.22	76.46	78.67	76.04
90	54.46	54.42	52.94	65.84	66.63	64.00
100	43.31	43.00	42.18	53.37	53.25	51.22
120	30.78		30.66			35.45
150	23.71		24.05			27.65
200	22.97	22.56	21.13	25.41	25.69	24.42
300		17.01	17.86	21.16	20.60	20.3
400	17.96	17.78	17.40	20.91	20.87	20.07
500		16.68	17.16	20.67	20.77	20.44
600	17.34	17.89	17.27	21.27	22.21	21.17
700		16.97	17.58	21.92	22.74	21.82
800		17.15	17.81	22.47	23.01	22.06
900	18.44	18.32	17.60	22.71	23.01	21.96
1000		18.37	17.70	22.55	22.74	21.73
1200				21.76		20.44
1400	18.65		17.39			19.21
1500				20.15		18.86
1800	17.67	17.52	16.01	19.44	19.27	17.85
2000		17.11		19.09	19.00	17.00
2450	14.81		13.04	17.18		15.17
3000	12.47	14.60	10.97	15.66	16.86	13.65

Table 3. NORMAN – SAR ($\mu\text{W kg}^{-1}$ for 1 V m^{-1}) for various assumptions of skin and fat properties.

HPA calculations						
MHz	fat infiltrated with blood			fat not infiltrated with blood		
	wet skin	average dry/wet	dry skin	wet skin	average dry/wet	dry skin
400	17.40	17.35	17.31	17.63	17.58	17.53
600	17.27	17.19	17.11	17.49	17.39	17.31
900	17.60	17.53	17.45	18.07	17.97	17.87
1400	17.39	17.50	17.56	18.26	18.35	18.39
1800	16.01	16.33	16.60	17.05	17.42	17.73
2450	13.04	13.52	13.97	13.65	14.23	14.79
3000	10.97	11.36	11.77	11.07	11.53	12.04

Table 4. NORMAN – SAR ($\mu\text{W kg}^{-1}$ for 1 V m^{-1}) for various assumptions of skin and fat properties at 1800 MHz. Percentage differences from wet skin, fat infiltrated with blood are given in brackets.

	fat infiltrated with blood			fat not infiltrated with blood		
	wet skin	average dry/wet	dry skin	wet skin	average dry/wet	dry skin
HPA	16.01	16.33 (2.0%)	16.6 (3.7%)	17.05 (6.5%)	17.42 (8.8%)	17.73 (10.7%)
NICT	17.53	17.77 (1.4%)	18.01 (2.7%)	18.60 (6.1%)	18.89 (7.8%)	19.16 (9.3%)
NIT	16.82	17.07 (1.5%)	17.31 (2.9%)	18.00 (7.0%)	18.28 (8.7%)	18.42 (9.5%)

Table 5. NORMAN – SAR ($\mu\text{W kg}^{-1}$ for 1 V m^{-1}) for various SAR algorithms.

f, MHz	SAR algorithms			
	A	B	C	D
100	42.18	42.61	42.09	42.41
400	17.40	17.51	17.75	17.86
900	17.60	17.77	18.32	18.47
1800	16.01	16.22	17.08	17.28
2450	13.04	13.34	14.48	14.72
3000	10.97	11.29	12.67	12.91

Table 6. NAOMI – SAR ($\mu\text{W kg}^{-1}$ for 1 V m^{-1}) using HPA dielectric properties and SAR algorithm A. Percentage differences from the HPA values are given in brackets.

f, MHz	HPA	NICT	NIT
900	21.96	21.93 (−0.1%)	21.56 (−1.8%)
1800	17.85	17.86 (+0.1%)	17.37 (−2.7%)
3000	13.65	14.53 (+6.4%)	13.38 (−2.0%)

Figure 1. Whole-body averaged SAR in TARO calculated at a resolution of 2 mm normalised to a mass of 65 kg under isolated conditions. The incident electric field is 1 V m^{-1} (r.m.s.).

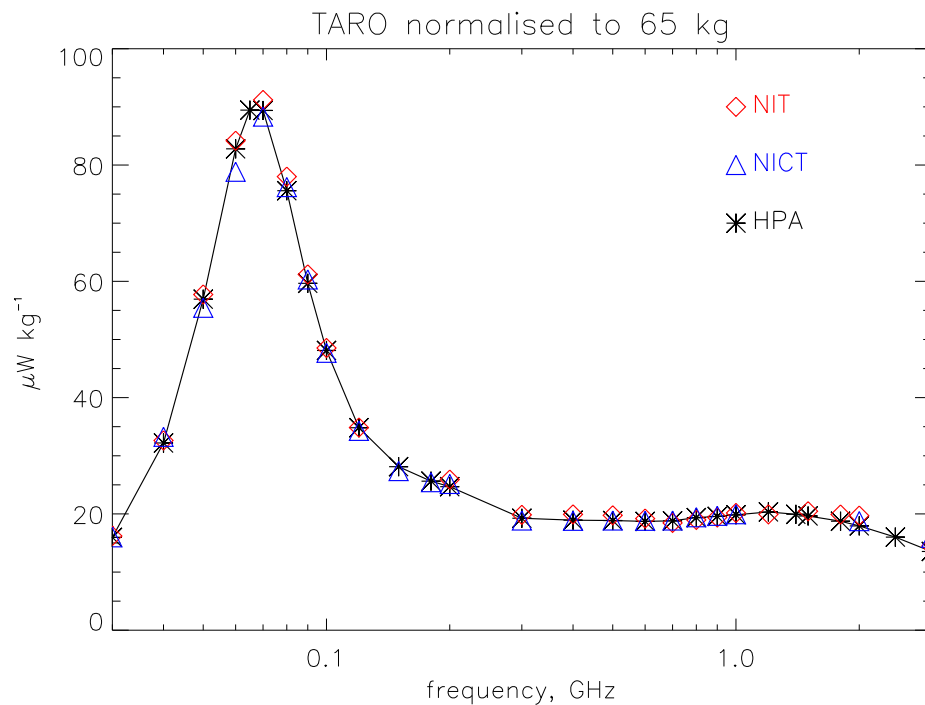


Figure 2. TARO – Percentage differences from the HPA whole-body averaged SAR values normalised to 65 kg.

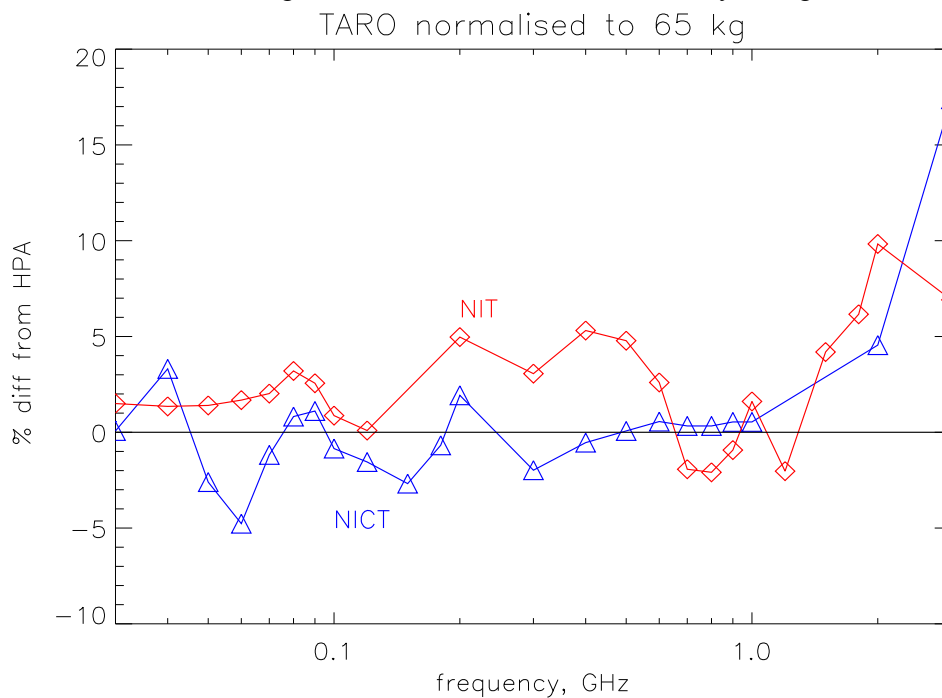


Figure 3. Whole-body averaged SAR in HANAKO calculated at a resolution of 2 mm normalised to a mass of 53 kg under isolated conditions. The incident electric field is 1 V m^{-1} (r.m.s.).

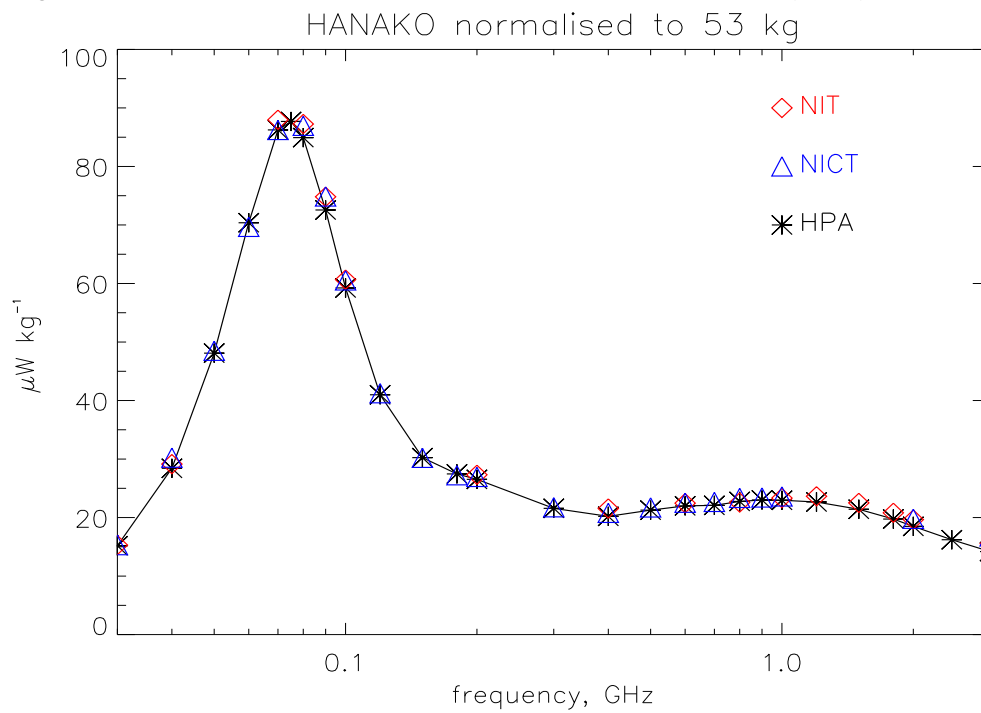


Figure 4. HANAKO – Percentage differences from the HPA whole-body averaged SAR values normalised to 53 kg.

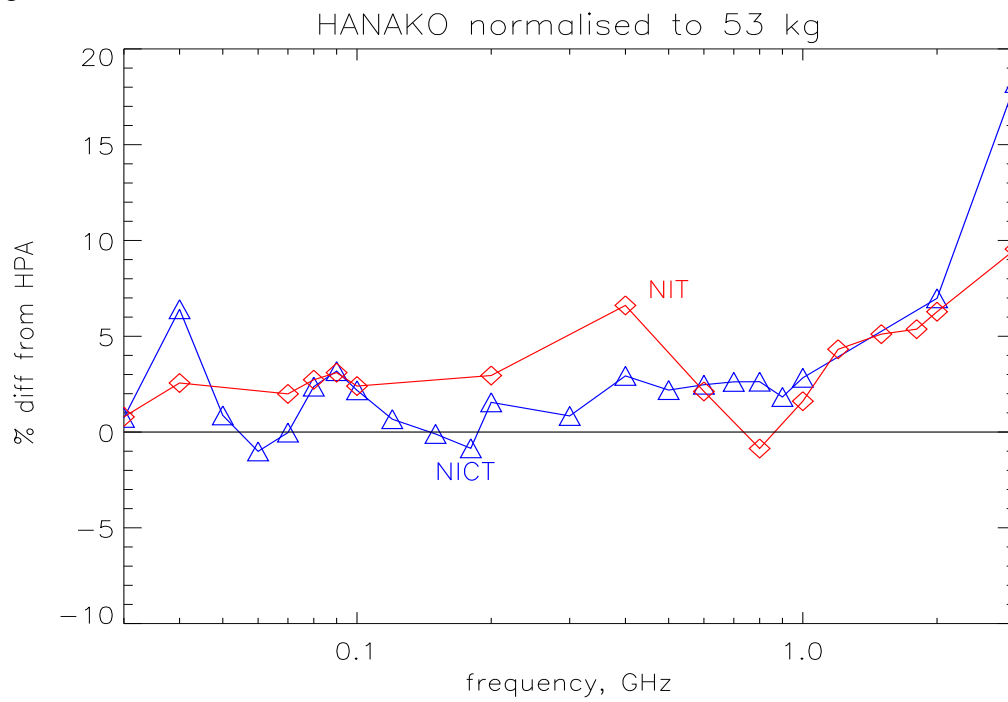


Figure 5. Comparison between NAOMI and HANAKO (HPA calculations). The incident electric field is 1 V m^{-1} (r.m.s.).

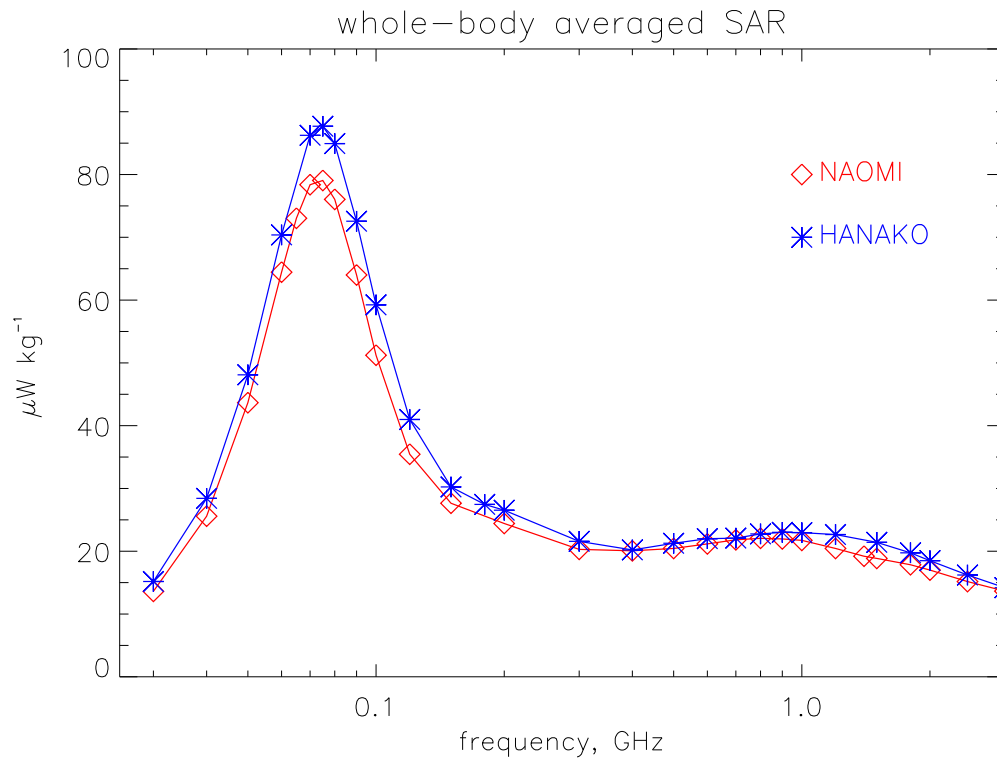


Figure 6. Comparison between NORMAN and TARO (HPA calculations). The incident electric field is 1 V m^{-1} (r.m.s.).

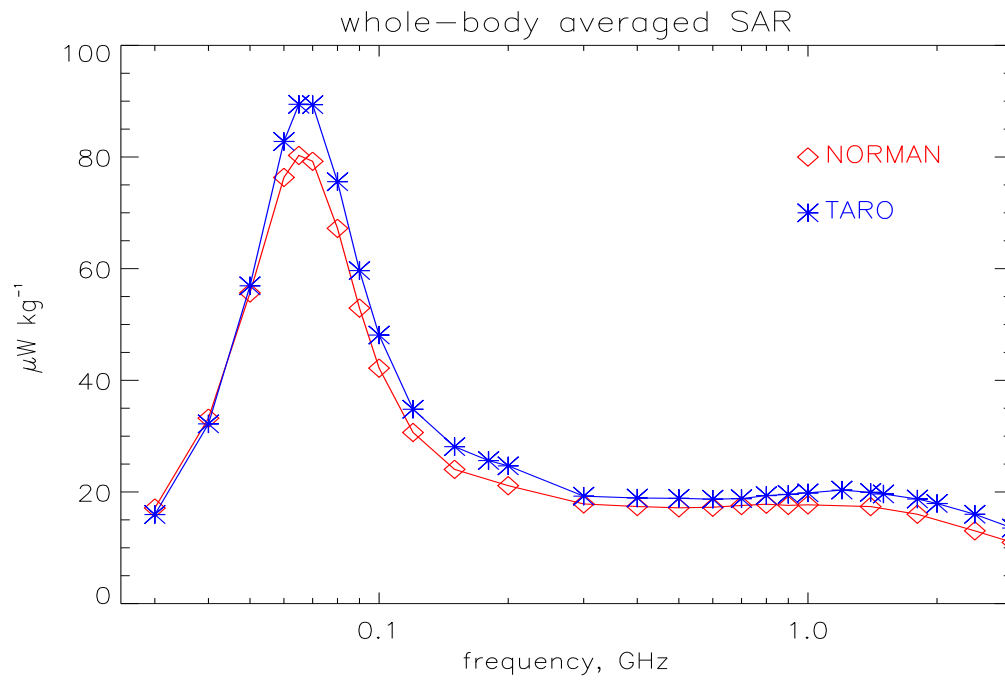


Figure 7. Whole-body averaged SAR in NORMAN calculated at a resolution of 2 mm normalised to a mass of 73 kg under isolated conditions. The incident electric field is 1 V m^{-1} (r.m.s.).

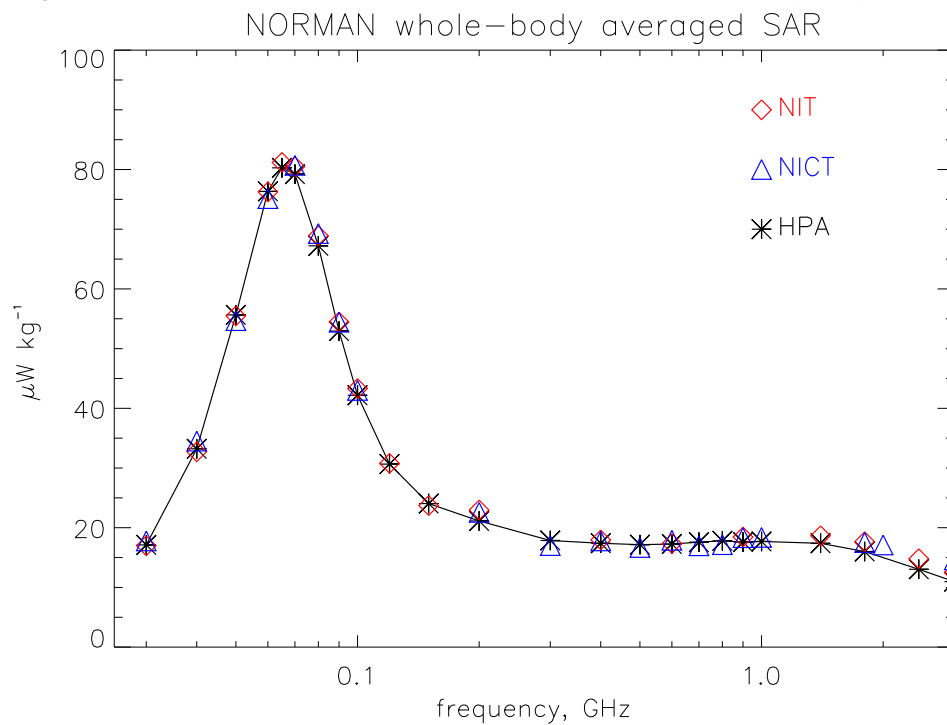


Figure 8. NORMAN – Percentage differences from the HPA whole-body averaged SAR values normalised to 73 kg.

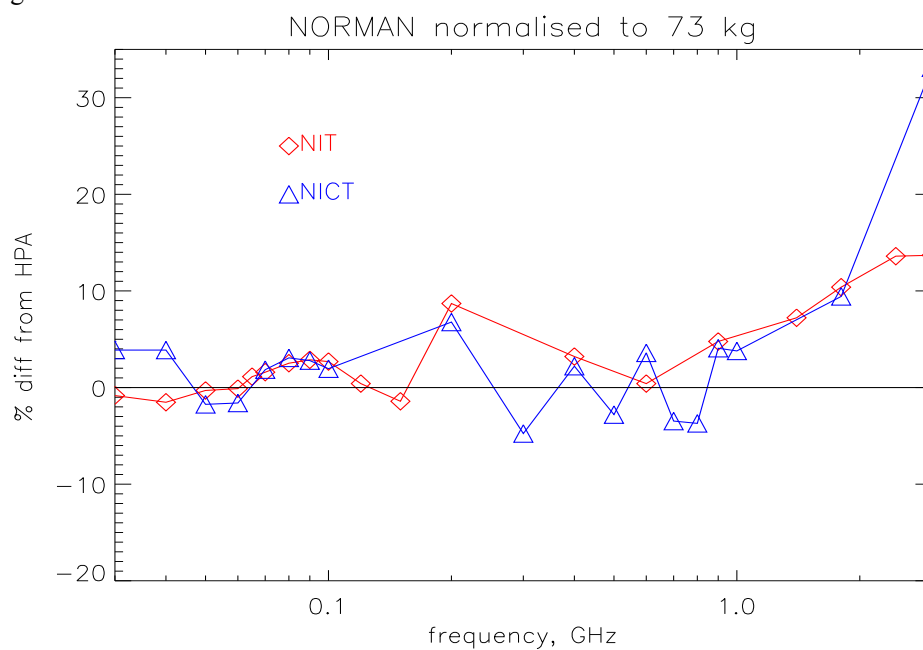


Figure 9. Whole-body averaged SAR in NAOMI calculated at a resolution of 2 mm normalised to a mass of 60 kg under isolated conditions. The incident electric field is 1 V m^{-1} (r.m.s.).

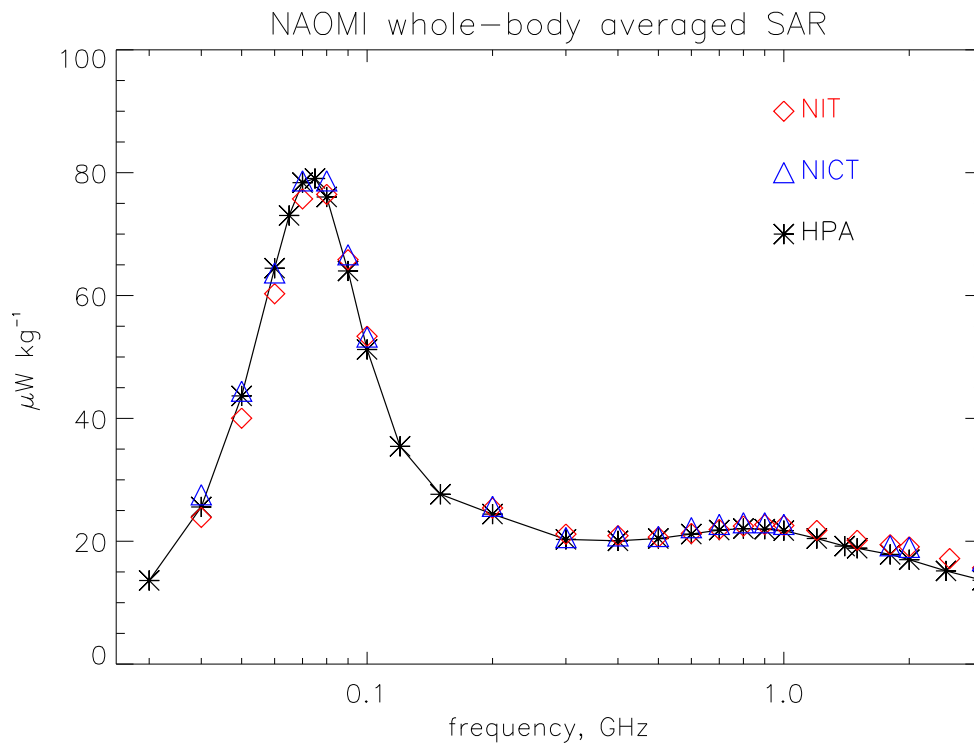


Figure 10. NAOMI – Percentage differences from the HPA whole-body averaged SAR values.

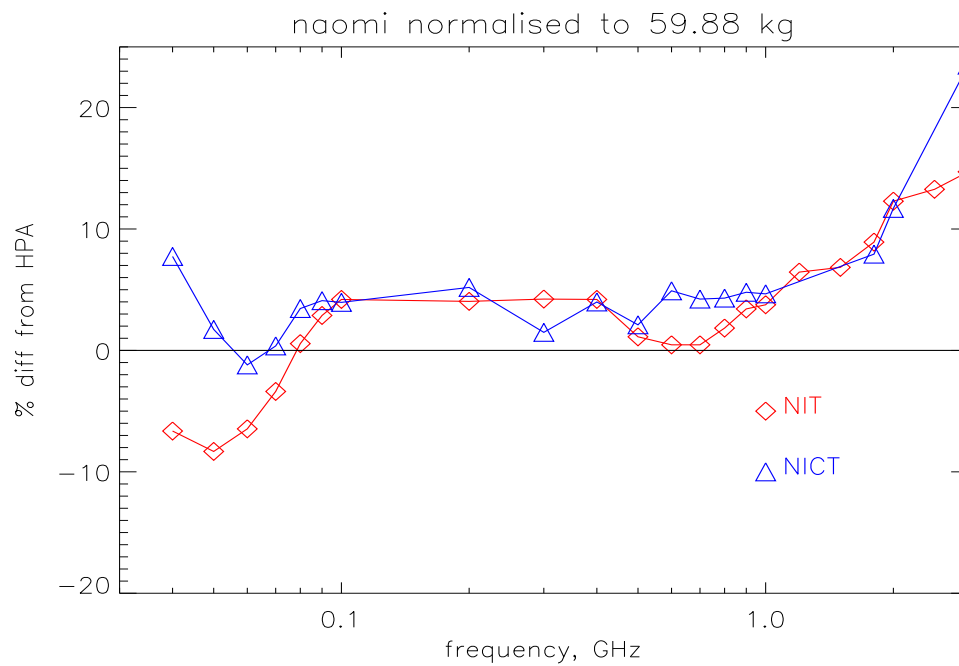


Figure 11. NORMAN – Percentage differences from the standard parameters of wet skin and fat infiltrated with blood.

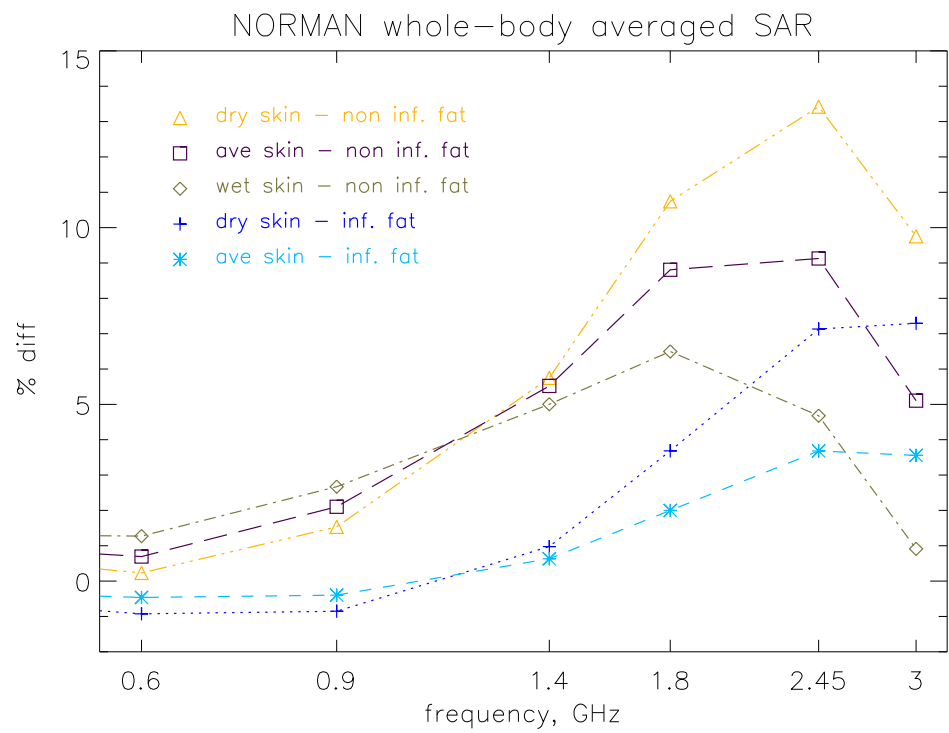


Figure 12. – Percentage differences from the standard algorithm A.

